


ORIGINAL ARTICLE

Gastric cancer–secreted exosomal X26nt increases angiogenesis and vascular permeability by targeting VE-cadherin

Xiaocui Chen¹ | Shuqiong Zhang¹ | Kun Du¹ | Naisheng Zheng¹ | Yi Liu¹ | Hui Chen¹ | Guohua Xie¹ | Yanhui Ma¹ | Yunlan Zhou¹ | Yingxia Zheng¹ | Lingfang Zeng² | Junyao Yang¹ | Lisong Shen^{1,3,4} 

¹Department of Clinical Laboratory, Xinhua Hospital, Shanghai Jiao Tong University School of Medicine, Shanghai, China

²School of Cardiovascular Medicine and Sciences, King's College – London British Heart Foundation Centre of Excellence, Faculty of Life Science and Medicine, King's College London, London, UK

³Faculty of Medical Laboratory Sciences, Shanghai Jiao Tong University School of Medicine, Shanghai, China

⁴Xin Hua Children's Hospital, Shanghai, China

Correspondence

Junyao Yang or Lisong Shen, Department of Clinical Laboratory, Xinhua Hospital, Shanghai Jiao Tong University School of Medicine, Shanghai 200092, China.
Email: yangjunyao@xinhuaemed.com.cn (JY); lisongshen@hotmail.com (LS)

Funding information

Key Specialty Development Program of Shanghai Municipal Health Commission; "Rising Stars of Medical Talent" Youth Development Program-Clinical Laboratory Practitioners Program, Grant/Award Number: 2019016; National Natural Science Foundation of China, Grant/Award Number: 81672363, 81802082 and 81873863; Gao Yuan Development Program of Shanghai Municipal Education Commission

Abstract

Angiogenesis is closely associated with tumorigenesis, invasion, and metastasis by providing oxygen and nutrients. Recently, increasing evidence indicates that cancer-derived exosomes which contain proteins, coding, and noncoding RNAs (ncRNAs) were shown to have proangiogenic function in cancer. A 26-nt-long ncRNA (X26nt) is generated in the process of inositol-requiring enzyme 1 alpha (IRE1 α)-induced unspliced XBP1 splicing. However, the role of X26nt in the angiogenesis of gastric cancer (GC) remains largely unknown. In the present study, we found that X26nt was significantly elevated in GC and GC exosomes. Then, we verified that X26nt could be delivered into human umbilical vein endothelial cells (HUVECs) via GC cell exosomes and promote the proliferation, migration, and tube formation of HUVECs. We revealed that exosomal X26nt decreased vascular endothelial cadherin (VE-cadherin) by directly combining the 3'UTR of VE-cadherin mRNA in HUVECs, thereby increasing vascular permeability. We further demonstrated that X26nt accelerates the tumor growth and angiogenesis in a mouse subcutaneous tumor model. Our findings investigate a unique intercellular communication mediated by cancer-derived exosomes and reveal a novel mechanism of exosomal X26nt in the regulation of tumor vasculature.

KEYWORDS

angiogenesis, exosomes, gastric cancer, noncoding RNAs, VE-cadherin

1 | INTRODUCTION

Gastric cancer (GC) is the fifth most common diagnosed cancer globally, and almost half of global GCs are diagnosed in East Asia.^{1,2}

Most patients with GC are in an advanced stage when first diagnosed, because of a lack of valid early diagnosis.^{3,4} Despite advances in both the diagnostic methods and various treatments for GC over the past decades, including surgery, chemotherapy, radiotherapy,

This is an open access article under the terms of the Creative Commons Attribution-NonCommercial-NoDerivs License, which permits use and distribution in any medium, provided the original work is properly cited, the use is non-commercial and no modifications or adaptations are made.

© 2020 The Authors. *Cancer Science* published by John Wiley & Sons Australia, Ltd on behalf of Japanese Cancer Association.

and immunotherapy, the overall 5-year survival rate for GC has not markedly improved.⁵⁻⁷ Therefore, the exploration of an effective therapeutic target is urgently needed.

Angiogenesis is essential for tumorigenesis, progression, invasion, migration, and metastasis by providing oxygen and nutrients.⁸ The steps of angiogenesis usually contain protease production, endothelial cell (EC) migration and proliferation, vascular tube formation, anastomosis of newly formed tubes, synthesis of a new basement membrane, and incorporation of pericytes and smooth muscle cells.^{9,10} Vascular endothelial cadherin (VE-cadherin) is a central component of the adherens junction of ECs.¹¹ Loss of the membrane-associated adhesion molecule will impair the endothelial junction integrity and increase vascular permeability. Current study indicated that VE-cadherin plays a vital role in angiogenesis.¹² In recent decades, many angiogenesis inhibitors, such as trastuzumab and apatinib have been suggested and approved for treatment.¹³ However, they do not show satisfactory outcomes because of an incomplete understanding of tumor angiogenesis. Therefore, investigating precise molecular mechanism involved in GC angiogenesis turns out to be crucial.

Exosomes, extracellular vesicles (EVs), ranging from 30 to 150 nm in diameter, are secreted by several types of cells.¹⁴ It has been shown that exosomes can transfer a variety of functional biological molecules, including proteins, coding, and noncoding RNAs (ncRNAs) into the extracellular space or biological fluids to mediate cell communication.^{15,16} Exosomes derived from cancer cells contain oncogenic information that induces the tumor microenvironment to be conducive to cancer development. Growing evidence indicated that exosomes can lead to cancer progression by mediating ncRNAs cross-talk between tumor cells and surrounding cells.^{17,18} Cancer-secreted exosomal ncRNAs can be transported to adjacent ECs and contribute to tumor angiogenesis.^{19,20} However, the mechanisms underlying the effects of ncRNAs on the cancer are still poorly understood.

Endoplasmic reticulum (ER) stress/the unfolded protein response (UPR) activation has been identified to be related to tumor progression.²¹ The IRE1a-XBP1 pathway is a conserved adaptive mediator of the UPR. Upon activation, the endoribonuclease domain of inositol-requiring enzyme 1 alpha (IRE1 α) cleaves unspliced XBP1 (XBP1u) mRNA and removes a 26-nt-long ncRNA (X26nt), which generates a spliced XBP1 (XBP1s) encoding an active transcription factor.¹⁴ Our previous studies have shown that XBP1 splicing can increase endothelial nitric oxide synthase expression and cellular location, leading to ECs migration and therefore contributing to wound healing and angiogenesis.²² Numerous studies have suggested that XBP1s plays pivotal roles in ECs proliferation, autophagy, and apoptosis.²³⁻²⁵ However, the function of X26nt has not been elucidated so far.

In the current study, we found that X26nt was apparently up-regulated in GC and exosomes derived from GC. We further verified that X26nt could be delivered into human umbilical vein endothelial cells (HUVECs) via GC cell exosomes and promoted the proliferation, migration, and tube formation of HUVECs. In addition, we confirmed

that X26nt could reduce the expression of VE-cadherin via binding to the 3'UTR of VE-cadherin mRNA. Our *in vivo* study also demonstrated that X26nt facilitated the tumor growth and angiogenesis in a mouse subcutaneous tumor model. These findings provided novel mechanistic insights for GC angiogenesis.

2 | MATERIALS AND METHODS

2.1 | Human serum and tissues

We obtained gastric tumor serum and tissues from patients with GC at Xinhua Hospital, Shanghai Jiao Tong University School of Medicine (Shanghai, China). GC tissue chip containing 16 pairs of tumor tissues and paracancerous tissues were obtained from Shanghai Outdo Biotech Company. All patients were diagnosed and staged by pathological analyses based on the TNM criteria defined by the International Union against Cancer (UICC). The study protocol conformed to the ethical guidelines of the Declaration of Helsinki and was approved by the Institutional Review Board and Ethics Committee of Xinhua Hospital.

2.2 | Cell culture

The GC cell line BGC-823 cells (BGCs), MGC-803 cells, MKN-45 cells, and GES-1 cells were purchased from the Cell Bank of Type Culture Collection of the Chinese Academy of Sciences and cultured in Dulbecco's Modified Eagle's Medium (DMEM; Gibco, Life Technologies) with 10% FBS and antibiotics (100 IU/mL penicillin and 100 μ g/mL streptomycin). HUVECs were obtained from ScienCell Research Laboratories and cultured in basal endothelial cell medium (EBM2) supplemented with the EGM-2-MV bullet kit (CC-3156; Lonza). The cell culture was placed in humidified air at 37°C with 5% CO₂.

2.3 | RNA extraction and quantitative real-time PCR (qRT-PCR)

Total RNA was extracted using RNeasy Mini Kit (QIAGEN) according to the manufacturer's instructions. The concentration and quality of the total RNA were assessed with Nanodrop Spectrophotometer (Thermo Fisher Scientific). The cDNA synthesis was performed using Prime-Script RT master mix (TaKaRa). Primers were obtained from Shanghai Sangon. qRT-PCR analysis was performed in triplicate on 7900 HT Real-Time PCR System (Applied Biosystems) using SYBR Premix Ex Taq (TaKaRa). Relative expression was calculated using U6 as an endogenous internal control. The U6 sense primer was 5'-TGGAACGCTTCACGAATTTGCG-3' and the antisense primer was 5'-GGAACGATACAGAGAAGATTAGC-3'. The X26nt primers are as follows: the outer primer used for primary amplification was 5'-GGTTTTCCAGTCACGACGCTGCACTCAGACTAC-3' and 5'-CAG

CTATGACCATGATTACGCAGAGGTGCAC-3'; the second-round amplification using inner primer was 5'-GGTTTTCCAGTCACGACG-3' and 5'-CAGCTATGACCATGATTACG-3'.

2.4 | Fluorescence in situ hybridization

Fluorescence in situ hybridization (FISH) for X26nt and XBP1 probe was conducted as previously described.²⁶ GC tissues were fixed with 4% paraformaldehyde, using FAM-labelled probe for X26nt (5'-FAM-AGAGGTGCACGTAGTCTGAGTGCT GC-3') and Cy3-labelled probe for XBP1 (5'-Cy3-GGGGTGACAACCTGGGCCTGCACCTGC-3') at 8 ng/ μ L concentration. Hybridization was performed at 37°C overnight. Slides were subsequently counterstained using DAPI. Images were visualized using Leica SP5 Laser scanning confocal microscope.

2.5 | Exosome isolation and analysis

BGCs were incubated for 48 hours in DMEM medium with free FBS. This conditioned medium was collected and the exosomes were isolated using exoEasy Maxi Kit (cat. no. 76 064, QIAGEN) according to the manufacturer's instructions. Then, the identification of the exosomes was processed according to the protocol described in Exosome Antibody Array (System Biosciences). For exosome uptake experiments, exosome preparations were labeled with PKH67 Fluorescent Cell Linker Kits (Sigma-Aldrich) according to the manufacturer's instructions, followed by washing through Exosome Spin Columns (MW3000; Invitrogen) to remove excess dye. Then, the exosomes were incubated with HUVECs for 12 hours and examined under a SP5 confocal microscope (Leica).

2.6 | Transmission electron microscopy (TEM)

The exosomes were suspended with 50-100 μ L 2% paraformaldehyde, then 10 μ L of exosome suspension was absorbed onto Formvar carbon-coated copper grids (200 mesh) for 1 min. After washing with PBS, 1% glutaraldehyde was added to copper grids for 5 min. Samples were washed with double-distilled water and negatively stained with 2% uranyl acetate solution for 1 min. Subsequently, 50 μ L methylcellulose was added to the samples for 5 min on the ice. After air dry, the samples were visualized at 87 000 \times in a Philips Tecnai transmission electron microscope at 80 kV.

2.7 | Nanoparticle tracking analysis

Isolated exosome samples were appropriately diluted using 1 \times PBS buffer to measure the particle size and concentration. The exosome particle size and concentration were measured using nanoparticle tracking analysis (NTA) with ZetaView PMX 110 (Particle Metrix) and

corresponding software ZetaView 8.04.02. NTA measurement was recorded and analyzed at 11 positions. The ZetaView system was calibrated using 110 nm polystyrene particles. The temperature was maintained around 23 and 37°C.

2.8 | Western blot

The equal amounts of protein extracts were separated through an 10% sodium dodecyl sulfate-polyacrylamide gel (SDS-PAGE) and then transferred to a PVDF membrane (IPFL00010; Merck Millipore). Then, the membranes were incubated with Anti-VE-cadherin antibody (1:500; ab166715; Abcam) and Anti-mouse IgG (H + L; DyLight² 680 Conjugate; #5470; Cell Signaling Technology). GAPDH was used as endogenous control, and the densitometry analysis was performed with ImageJ software (NIH).

2.9 | Transfection assay

For in vitro transfection of X26nt mimics, X26nt inhibitors (X26nt asRNA), Cy3-labeled X26nt, X26nt-overexpressing (X26nt OE) lentivirus, and negative control (Sangon/GeneChem) were transfected using Lipofectamine 3000 (Life Technologies) according to the manufacturer's instructions. Transfection cells were collected and used for further analysis after 24 or 48 hours.

2.10 | Cell proliferation assay

Cell proliferation assay was performed in vitro according to the manufacturer's guidelines (C0071S, Beyotime). The cells were photographed using an Olympus CKX53 Imaging System (Olympus Corporation) with an excitation wavelength of 495 nm.

2.11 | Wound healing assay

Different pretreated HUVECs were seeded at a density of 2.0×10^5 cells/mL in a six-well plate, and cells were allowed to adhere on the plate overnight. Then wounds were made using a 1 mL pipette tip, and the wells were washed with PBS to remove debris. Cells were cultured in fresh media containing 2% FBS. Photographs were taken using an Olympus IX71 Imaging System (Olympus Corporation) at 0 and 12 hours respectively. The experiments were carried out three times.

2.12 | Cell migration and tube formation assays

Cell migration and tube formation assays were performed in vitro according to standard protocols, as described previously.²² All experiments were performed in triplicate.

2.13 | In vitro detection of X26nt transfer

To further observe the transfer of X26nt, exosomes derived from BGCs transfected with Cy3-labelled X26nt or without transfection were added to HUVECs culture medium. After 24 hours, the HUVECs were fixed with 4% paraformaldehyde for 30 min, treated with 0.1% Triton X-100 for 10 min, and blocked with 1% BSA for 1 hour at room temperature. F-actin was stained with Alexa 488 phalloidin (1:1000, Life Technologies) according to the manufacturer's guidelines. Cells were mounted with ProLong® Gold antifade Reagent with DAPI (Life Technologies). Images were captured using Leica SP5 Laser scanning confocal microscope.

2.14 | Immunofluorescence

The immunofluorescence was performed by staining with a rabbit polyclonal antibody against human/mouse VE-Cadherin (1:200; ab33168, Abcam) and a Goat Anti-Rabbit IgG H&L (Alexa Fluor 488) (1:200; ab150077, Abcam) as previously described.²⁷ Then cells were mounted with ProLong® Gold antifade Reagent with DAPI (Life Technologies). Images were captured using Leica SP5 Laser scanning confocal microscope.

2.15 | Transendothelial migration assay

The transendothelial migration was performed as previously described.²⁸ All experiments were performed in triplicate.

2.16 | Luciferase reporter assay

Wild-type and mutated VE-cadherin 3'UTRs were synthesized and cloned into pmirGLO vector (luciferase report vector, Promega). HEK293 cells were seeded at 1×10^5 cells per well in 24-well plates the day prior to transfection. Cells were transfected with pmirGLO luciferase expression construct containing the 3'UTR of target gene, pRL-TK Renilla luciferase vector (Promega), and mimics or negative control RNA (Ambion). After 48 hours transfection, luciferase activities were measured using the Dual-Luciferase Reporter Assay System (Promega) and normalized to Renilla luciferase activity. All experiments were performed in duplicate with data pooled from three independent experiments.

2.17 | Immunohistochemistry

Immunohistochemical assay was performed as described previously.²⁹ The tumor tissues were fixed in 4% paraformaldehyde, embedded in paraffin, sectioned, and then stained with anti-CD31 (ab28364; Abcam) antibody. Images were captured under a light microscope.

2.18 | In vivo tumor xenografts

In vivo studies, 4-6-week-old male BALB/c nude mice were purchased from Shanghai Laboratory Animal Center of China. Briefly, BGCs transfected with X26nt OE lentivirus and control lentivirus were subcutaneously injected into nude mice. Another group received subcutaneous injections of BGCs, and we injected 15 μ g of pCMV-X26nt asRNA and empty pCMV vector control to the tumors every other day when visible tumors appeared. The mice were examined at regular times until they were sacrificed. The tumor size was measured using digital caliper, and the tumor volume was calculated with the following formula: volume = $0.5 \times \text{width}^2 \times \text{length}$. All animal procedures were carried out with the approval of the Institutional Committee of Shanghai Jiao Tong University School of Medicine for Animal Research.

2.19 | Statistical analysis

Statistical significance was assessed using unpaired sample *t* tests for comparison between two groups and one-way ANOVA for comparison among multiple groups. $P < .05$ was considered significant. Statistical analysis was performed using GraphPad Prism Version 8.0 (GraphPad Software, Inc).

3 | RESULTS

3.1 | X26nt is obviously upregulated in GC

XBP1 splicing has been associated with the initiation and progression of tumors. XBP1 splicing product X26nt was first examined in tumor serum from hepatoma cancer, colon cancer, breast cancer, and GC patients. We found that the levels of X26nt were remarkably higher in GC serum than others (Figure 1A). Then, we checked the X26nt level of GC and normal serum exosomes and found that the X26nt levels of GC serum exosomes were higher than those of normal serum exomes (Figure 1B). Besides, the expression level of X26nt was significantly higher in GC tissues than in adjacent tissues (Figure 1C,D). These results indicated that the level of X26nt was upregulated in GC.

3.2 | Exosomes derived from GC cells can be ingested by HUVECs

To confirm whether GC cell-derived exosomes play a pivotal role in the progress of GC, we isolated exosomes from the conditioned medium of BGCs and observed them with TEM (Figure 2A). Nanovesicles with a diameter of 30-150 nm were found in exosomes purified from BGCs (Figure 2B). Meanwhile, exosomal markers including CD63, Hsp70, CD9, CD81, and TSG101 were observed using Western blot (Figure 2C). Furthermore, to verify

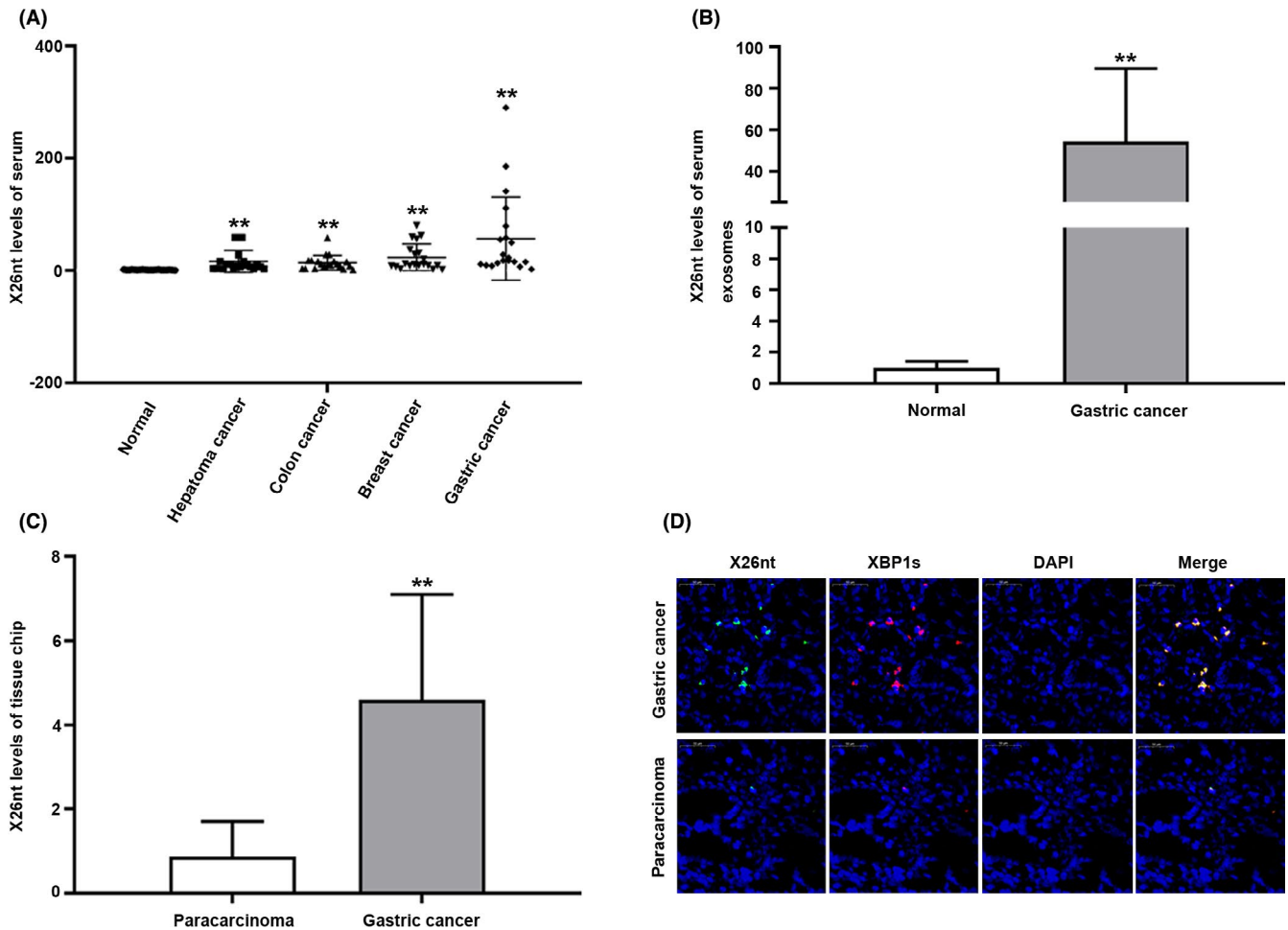


FIGURE 1 X26nt is highly expressed in gastric cancer (GC). A, qRT-PCR analysis of X26nt expression in normal, hepatoma cancer, colon cancer, breast cancer, and GC serum ($n = 20$), $**P < .01$. B, qRT-PCR analysis of X26nt expression in GC and normal serum exosomes ($n = 16$), $**P < .01$. C, Expression of X26nt in paracancerous and GC tissue chip ($n = 16$), $**P < .01$. D, FISH of X26nt and spliced XBP1 (XBP1s) in paracancerous and GC tissues ($n = 16$)

whether BGC-secreted exosomes can be taken up by HUVECs, HUVECs were cocultured with BGC exosomes stained with PKH67. Confocal microscopy was used to detect uptaken PKH67-labeled exosomes in HUVECs (Figure 2D).

3.3 | Effects of exosomes on angiogenesis in vitro

To demonstrate the role of GC exosomes in angiogenesis, we examined the proliferation of HUVECs by EdU assay, detected the migration of HUVECs by wound healing assay and transwell assay, and conducted a tube formation assay of HUVECs. We knocked down exosomal X26nt via transfecting BGCs with X26nt inhibitors which are X26nt antisense RNA (X26nt asRNA) plasmid to delete X26nt from the exosomes (exo-X26nt-del; Figure S1). We found that BGC exosomes obviously promoted the proliferation of HUVECs, while this effect was not obvious when HUVECs were cocultured with exosomes from which X26nt was deleted (Figure 3A,B). As expected, coculturing with BGC exosomes significantly increased the migration of HUVECs. However, after X26nt was deleted,

BGC exosomes showed no marked effect (Figure 3C-F). To further investigate the effects of BGC exosomes on EC tube formation, HUVECs were treated with BGC exosomes or exo-X26nt-del. The branch points of the tube-like structure in the HUVECs cocultured with BGC exosomes were significantly increased, while exo-X26nt-del attenuated this promotion (Figure 3G,H). A similar phenomenon was observed in MGC-803 cells (Figure S2). In a word, our findings indicated that exosomes from BGCs had a positive effect on angiogenesis.

3.4 | X26nt was validated to promote angiogenesis directly

To further verify the role of X26nt in angiogenesis, we investigated the proliferation, migration, and tube formation of HUVECs transfected with X26nt mimics (M.X26nt) or inhibitors (X26nt asRNA). The results showed that M.X26nt remarkably promoted, while X26nt asRNA suppressed the proliferation of HUVECs (Figure 4A,B). We also found that overexpressing X26nt prominently elevated

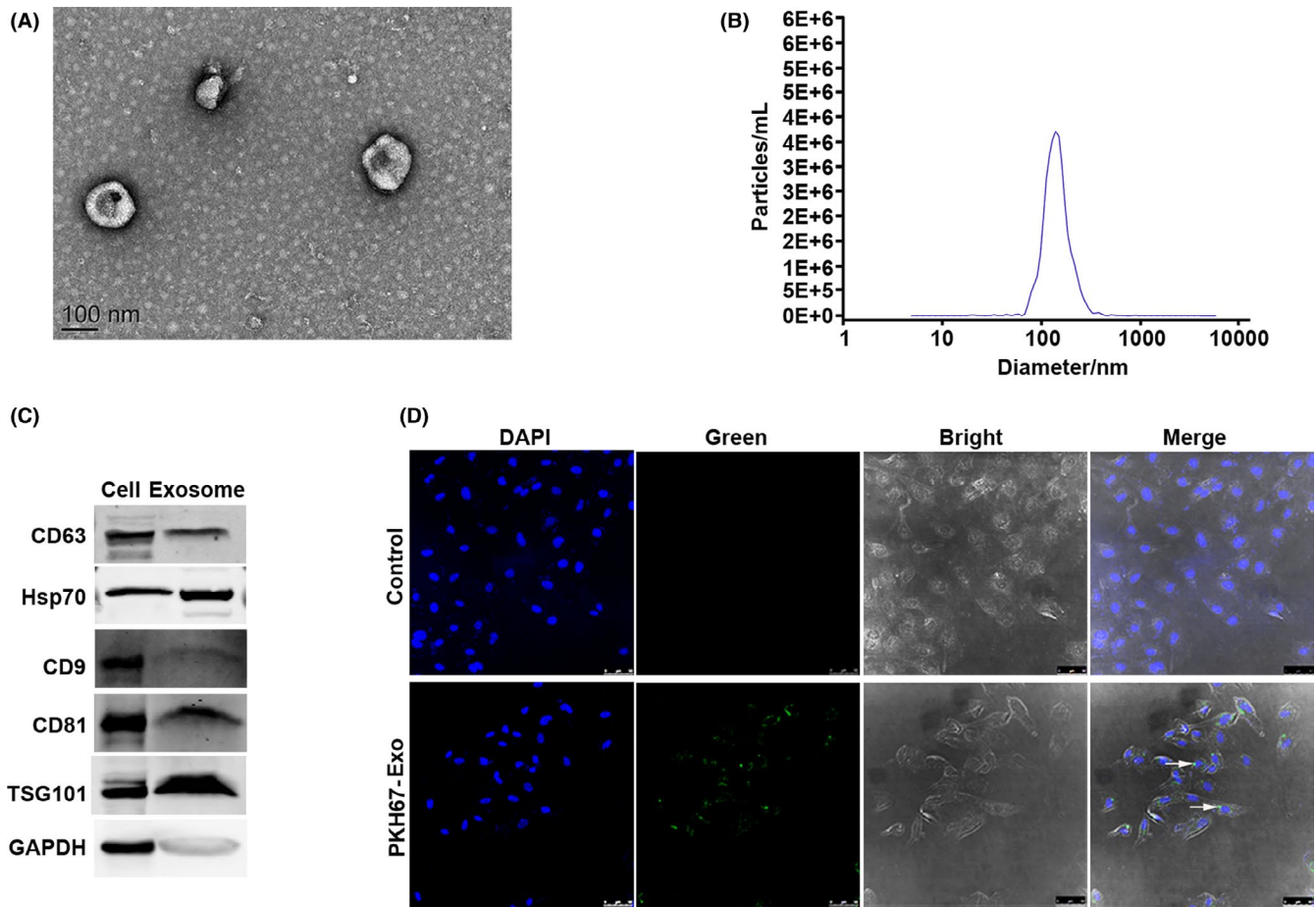


FIGURE 2 Exosomes derived from gastric cancer (GC) cells can be internalized by human umbilical vein endothelial cells (HUVECs). A, Representative transmission electron microscopy image of exosomes derived from BGC-823 cells (BGCs) (scale bar, 100 nm). B, Particle diameter (nm) of the purified exosomes. C, Western blot of exosome markers of BGC cellular protein and corresponding exosomes. D, Exosomes from BGCs can fuse with HUVECs. DAPI and PKH67 were used to stain HUVECs and exosomes, respectively, and PKH67-labelled exosomes were shown to enter HUVECs at 12 h. Arrows refer to PKH67-labelled exosomes (scale bar, 50 μ m; n = 3)

cell migration, while inhibition of the X26nt attenuated this effect (Figure 4C-F). Consistently, the branch points of the tube-like structure in the HUVECs were also promoted by M.X26nt, while it was restrained by X26nt asRNA (Figure 4G,H). Collectively, these results further demonstrated that the X26nt derived from BGC exosomes promoted angiogenesis.

3.5 | Exosomal X26nt is delivered to ECs and inhibits the expression of VE-cadherin

Recent studies showed that exosomes had an ability to transfer functional miRNAs and proteins to adjacent ECs and mediated the regulation of vascular integrity.³⁰ Due to the similar length, we suspect that X26nt may play a similar role to miRNAs. GES-1 cells are normal gastric epithelial cells, and we measured the level of X26nt in exosomes that were purified from GES-1 cells and GC cell lines MKN-45, MGC-803, and BGCs. The results revealed that the level of X26nt in GC cell exosomes was significantly higher than that in GES-1 cell exosomes (Figure 5A), which indicated that exosomes are

potential carriers of X26nt in GC. Then, HUVECs were incubated with exosomes from BGCs by different treatments. As a result, the X26nt level was markedly decreased in HUVECs cocultured with BGC exo-X26nt-del (Figure 5B).

To further verify whether the elevated X26nt level in HUVECs was directly derived from GC cell exosomes instead of the ECs themselves, BGCs were transfected with either Cy3-labeled X26nt or negative control. After 24 hours, we isolated exosomes from conditioned media collected from the above BGCs and added them to HUVECs culture medium. Cy3 labeled signal was shown in the HUVECs incubated with exosomes from BGCs transfected with Cy3-labeled X26nt (Figure 5C). Furthermore, we found that BGC exosomes decreased the expression of VE-cadherin in HUVECs, while BGC exo-X26nt-del eliminated the inhibition (Figure 5D,E). Consistently, exosome treatment remarkably increased the permeability of the HUVECs monolayer, and BGC exo-X26nt-del abrogated the effect in the transwell FITC-dextran assay (Figure 5F). Similarly, the exosomes of BGCs increased the transendothelial migration of cancer cells, while BGC exo-X26nt-del weakened the increase (Figure 5G,H). In addition, we also observed that BGC exosomes

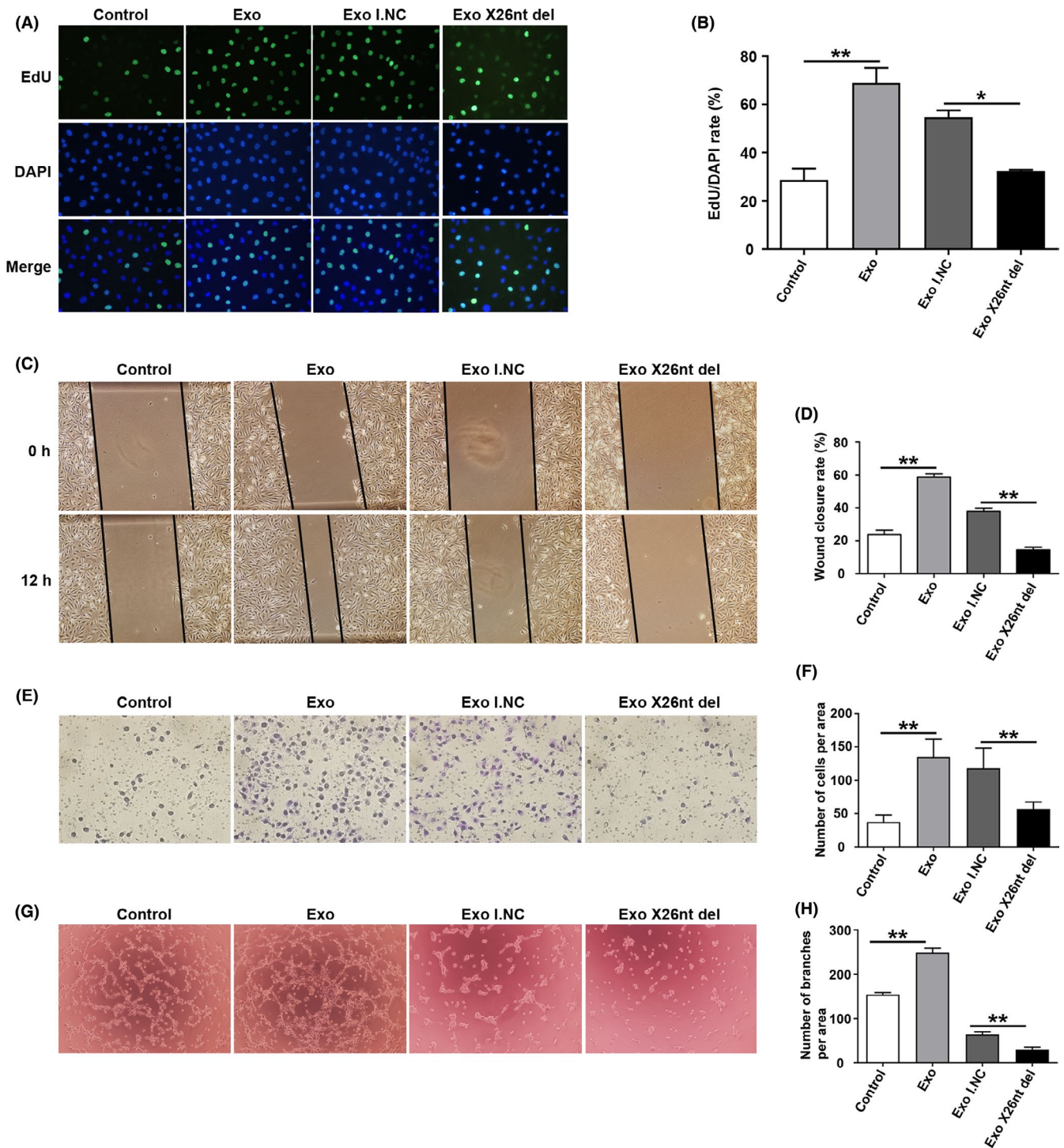


FIGURE 3 The role of exosomes in angiogenesis. Human umbilical vein endothelial cells (HUVECs) were incubated with exosomes isolated from BGC-823 cells (BGCs), and the proliferation, migration, and tube formation were examined after 24 h. To downregulate the level of exosomal (X26nt), we isolated exosomes from BGCs transfected with X26nt inhibitors (X26nt asRNA) for 24 h (exo X26nt del), and the scrambled X26nt inhibitors were transfected as control (exo I.NC). A, Proliferation of HUVECs measured by EdU assay (n = 3). B, Quantitative analysis EdU/DAPI rate of (A) (n = 3), * $P < .05$; ** $P < .01$. C, Migration of HUVECs measured by wound healing assay at 0 and 12 h (n = 3). D, Quantitative analysis wound closure rate of (C). Wound closure rate was defined as the percentage of the area occupied by the migrated cells to that of the empty area created by the scratching (n = 3), ** $P < .01$. E, Migration of HUVECs measured by transwell assay (n = 3). F, Quantitative analysis of migrated cells per area of (E) (n = 3), ** $P < .01$. G, Tube formation of HUVECs (n = 3). H, Quantitative analysis of branches per area of (G) (n = 3), ** $P < .01$

inhibited the expression of β -catenin which was connected to the cytoplasmic tail of VE-cadherin, while no effect was shown on P120 (Figure S3A,B). These data revealed that BGC-secreted exosomes

containing X26nt were internalized by vascular ECs and inhibited the expression of VE-cadherin, resulting in elevating vascular permeability.

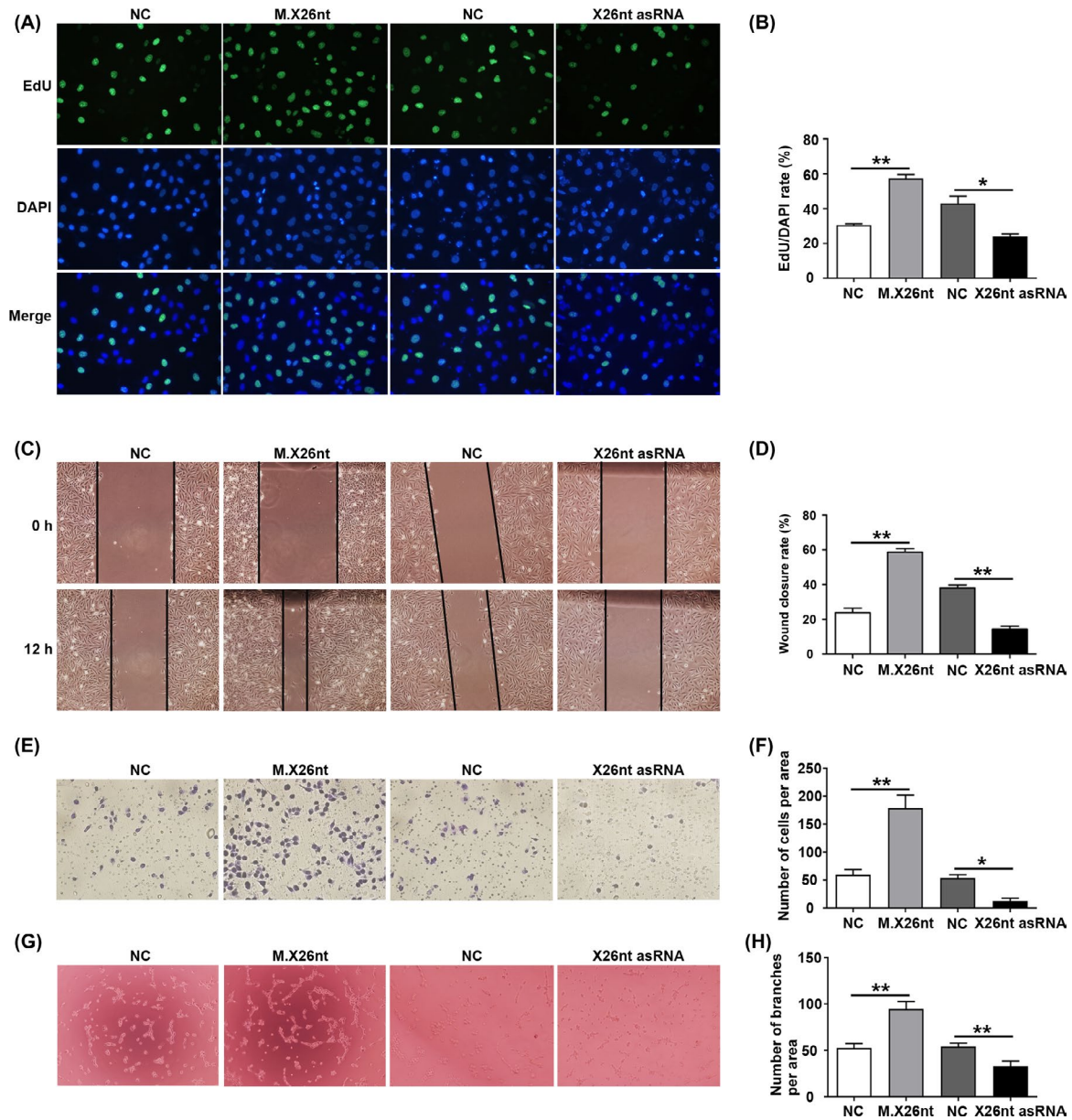
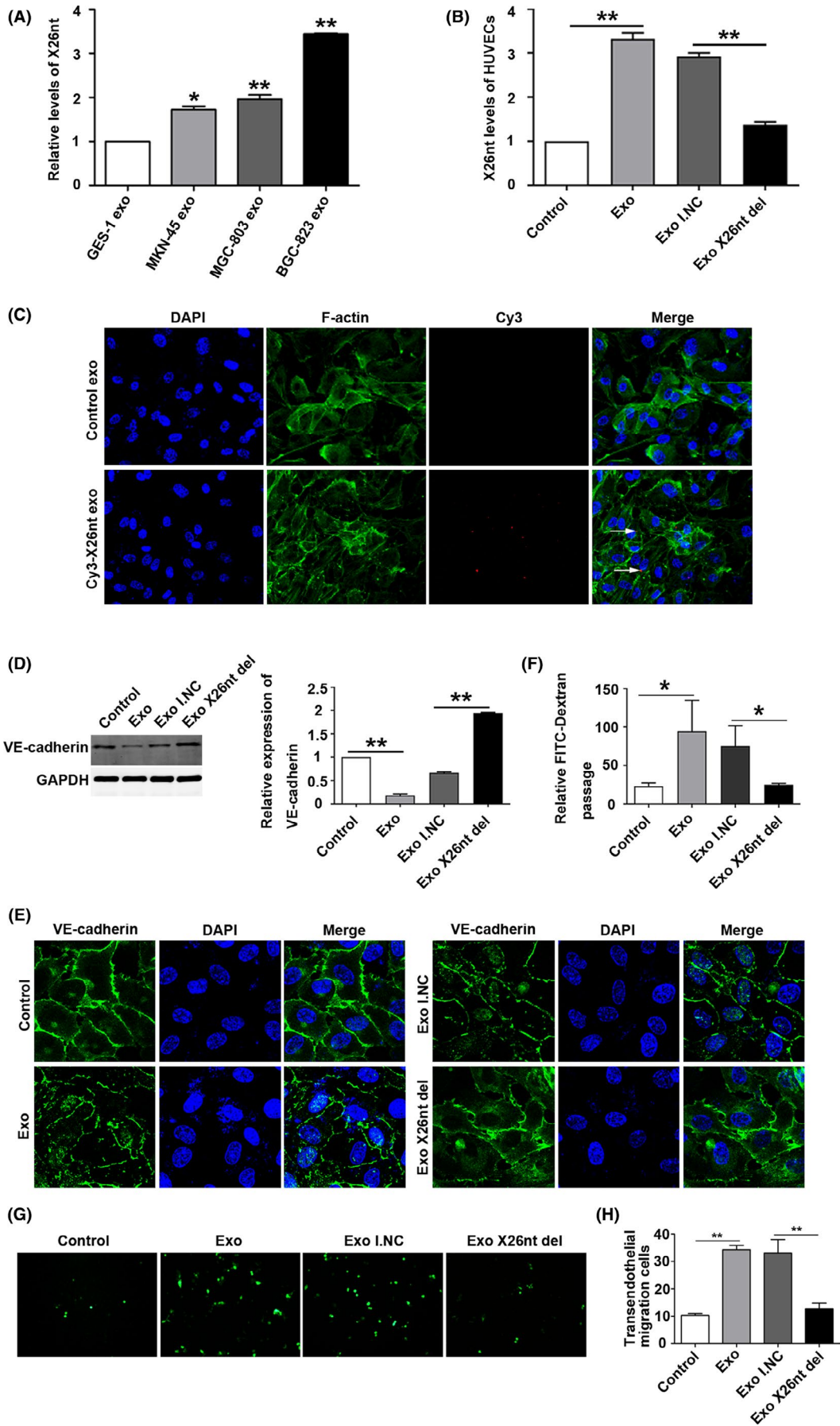


FIGURE 4 The role of X26nt in angiogenesis. Human umbilical vein endothelial cells (HUVECs) were transfected directly with X26nt mimics (M.X26nt) or inhibitors (X26nt asRNA), and the corresponding scrambled mimics and inhibitors were used as controls (NC). Subsequently, the proliferation, migration, and tube formation of HUVECs were examined at 24 h. A, Proliferation of HUVECs measured by EdU assay ($n = 3$). B, Quantitative analysis of (A) ($n = 3$), $*P < .05$; $**P < .01$. C, Migration of HUVECs measured by wound healing assay at 0 and 12 h ($n = 3$). D, Quantitative analysis of (C) ($n = 3$), $**P < .01$. E, Migration of HUVECs measured by transwell assay ($n = 3$). F, Quantitative analysis of (E) ($n = 3$), $*P < .05$; $**P < .01$. G, Tube formation of HUVECs ($n = 3$). H, Quantitative analysis of (G) ($n = 3$), $**P < .01$

FIGURE 5 X26nt derived from exosomes decreases the expression of vascular endothelial cadherin (VE-cadherin). A, Relative levels of X26nt in GES-1 cell exosomes, MKN-45 exosomes, MGC-803 exosomes, and BGC-823 exosomes by qRT-PCR ($n = 3$), $*P < .05$; $**P < .01$. B, The level of X26nt in human umbilical vein endothelial cells (HUVECs) cocultured with different exosomes were determined by qRT-PCR ($n = 3$), $**P < .01$. C, Exosomes derived from BGC-823 cells (BGCs) transfected with Cy3-labelled X26nt or without transfection (control) were added to HUVECs culture medium. HUVECs were fixed and stained with DAPI and Alexa 488 phalloidin. The fluorescence signal in HUVECs was detected by SP5 confocal microscope. Arrows refer to Cy3-labelled X26nt exosomes ($n = 3$). D, Immunoblots of VE-cadherin in HUVECs cocultured with different exosomes. GAPDH was presented as the loading control. Densitometric analysis of VE-cadherin/GAPDH ($n = 3$) is shown, $**P < .01$. E, Immunofluorescence of VE-cadherin in HUVECs cocultured with different exosomes ($n = 3$). F, Quantitative analysis of the FITC-dextran passage of HUVECs monolayer cocultured with different exosomes ($n = 6$), $*P < .05$. G, Green fluorescent protein-mouse forestomach carcinoma (GFP-MFC) cells were added to the top of HUVECs monolayer cocultured with different exosomes for 24 h that were grown on transwell inserts and incubated for another 12 h. The migratory GFP-MFC cells were captured using a fluorescent microscope ($n = 3$). H, Quantitative analysis of the migratory GFP-MFC cells of (G) ($n = 3$), $**P < .01$



3.6 | X26nt directly targets and inhibits the expression of VE-cadherin

We further explored how secreted X26nt attenuated the expression of VE-cadherin and increased vascular permeability. Using bioinformatic tools, we predicted the binding site of X26nt on VE-cadherin mRNA 3'UTR (Figure 6A). Then a dual-luciferase reporter assay revealed that cotransfection of M.X26nt significantly inhibited the activity of firefly luciferase reporter of wild-type 3'UTR of VE-cadherin mRNA, whereas this effect was abrogated when the predicted binding site in 3'UTR was mutated (Figure 6B). Furthermore, we detected the levels of VE-cadherin in the transfected cells. As predicted, cells overexpressing X26nt showed a low level of VE-cadherin (Figure 6C). However, transfection of X26nt

asRNA significantly attenuated the decrease of VE-cadherin in HUVECs (Figure 6D). Consistently, M.X26nt inhibited the expression of VE-cadherin in HUVECs monolayer, while treatment with X26nt asRNA significantly abolished the capacity of X26nt to decrease VE-cadherin (Figure 6E). These results suggested that GC cell-secreted exosomal X26nt may increase vascular permeability by directly targeting VE-cadherin.

3.7 | The role of X26nt in tumor growth and angiogenesis in vivo

To ascertain the role of X26nt in tumor growth and angiogenesis in vivo, we constructed a tumor-implanted model by subcutaneously

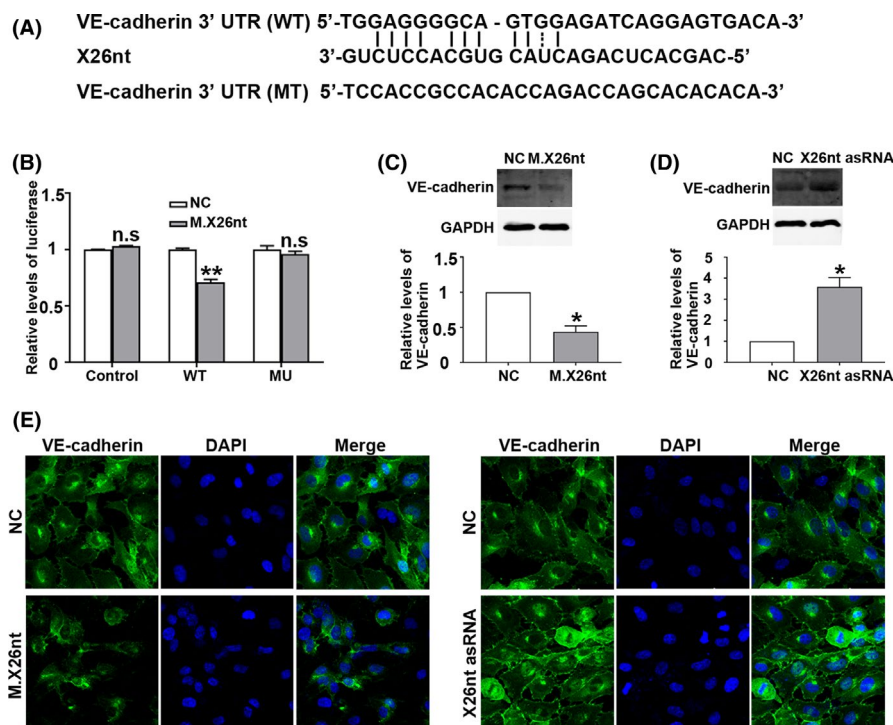
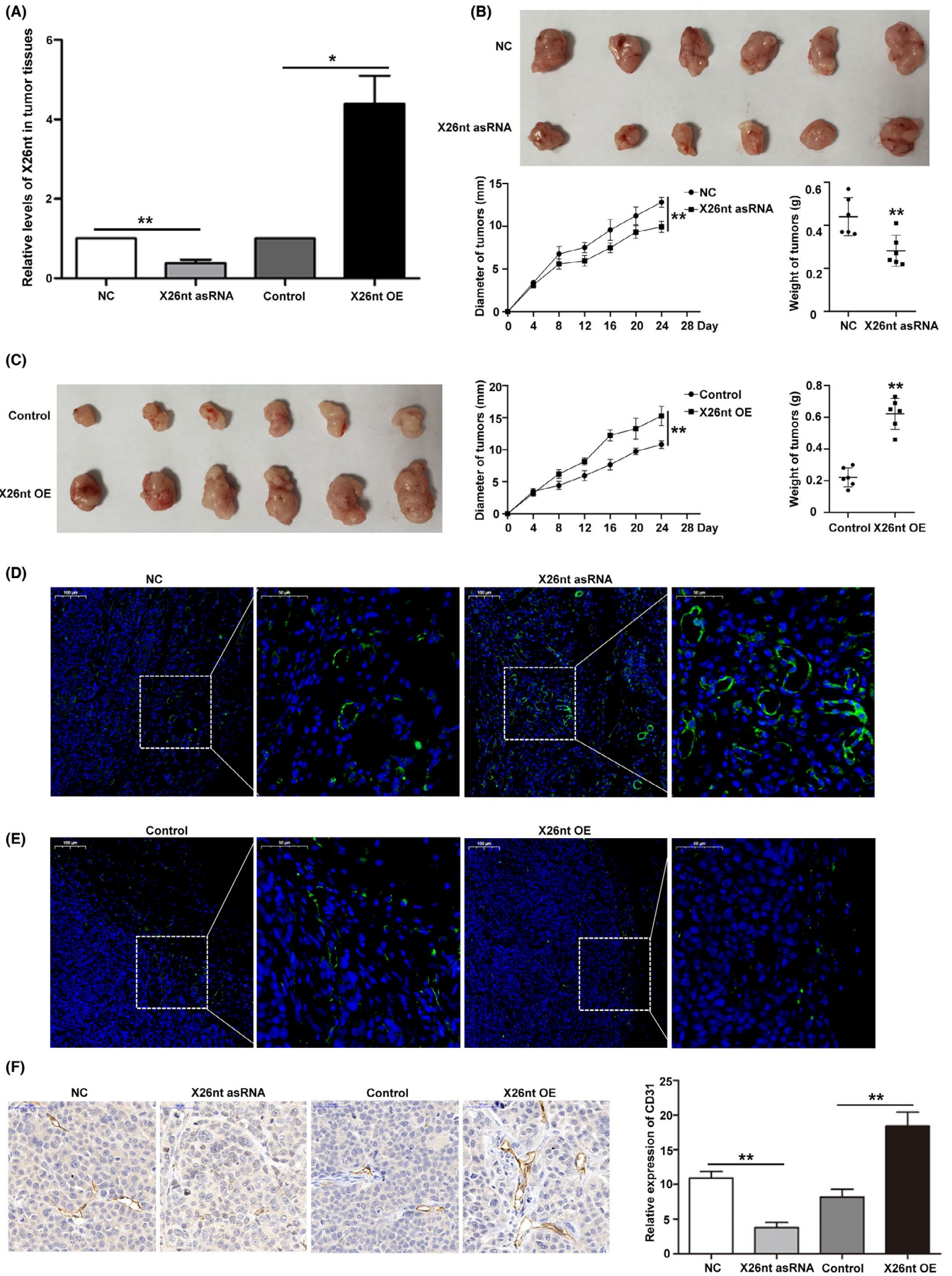


FIGURE 6 X26nt directly targets and inhibits vascular endothelial cadherin (VE-cadherin) expression. A, Schematic showing potential X26nt binding sites in the VE-cadherin mRNA 3'UTR. B, The luciferase assay of HEK293T cells cotransfected firefly luciferase reporter plasmid containing either wild-type (WT) or mutant VE-cadherin mRNA 3'UTR with M.X26nt ($n = 3$), $**P < .01$; n.s., nonsignificant. C, Western blot analysis of VE-cadherin expression in human umbilical vein endothelial cells (HUVECs) transfected with M.X26nt. GAPDH was presented as the loading control. Densitometric analysis of VE-cadherin/GAPDH ($n = 3$) is shown, $*P < .05$. D, Western blot analysis of VE-cadherin expression in HUVECs transfected with X26nt asRNA. GAPDH was presented as the loading control. Densitometric analysis of VE-cadherin/GAPDH ($n = 3$) is shown, $*P < .05$. E, Immunofluorescence staining of VE-cadherin in HUVECs transfected with M.X26nt and X26nt asRNA ($n = 3$)

FIGURE 7 The role of X26nt in tumor growth and angiogenesis in vivo. A, Relative levels of X26nt in different tumor tissues by qRT-PCR ($n = 6$), $**P < .01$; $*P < .05$. B, The BGC-823 cells (BGCs) were subcutaneously injected into the BALB/c nude mice to create a tumor-implanted model. When the tumor appeared, X26nt antisense RNA (X26nt asRNA) plasmid and mock control (NC) were injected to the tumor every other day before the mice were sacrificed. Analysis of tumor diameter and weight in each group ($n = 6$) is shown, $**P < .01$. C, The formed tumors from BGCs transfected with X26nt-overexpressing (X26nt OE) lentivirus and control lentivirus (control) were isolated and compared. Analysis of tumor diameter and weight in each group ($n = 6$) is shown, $**P < .01$. D, Immunofluorescence staining of vascular endothelial cadherin (VE-cadherin) in tumor treated with X26nt asRNA plasmid and NC ($n = 6$). E, Immunofluorescence staining of VE-cadherin in tumor of X26nt OE lentivirus and control ($n = 6$). F, Immunohistochemical staining of paraffin-embedded different tumor tissues with CD31 antibody ($n = 6$), $**P < .01$



injecting BGCs into the back of the armpit of nude mice. The levels of X26nt in tumor tissues were measured by qRT-PCR. X26nt levels were reduced in the X26nt knockdown group, while X26nt was increased in the X26nt OE group (Figure 7A). When visible tumor appeared, we injected X26nt asRNA plasmid and mock control (NC) to the formed tumor every other day to knock down X26nt until the mice were sacrificed. We found that knockdown X26nt inhibited the growth of tumor, and the diameter, weight, and volume were smaller than in the mock control (Figure 7B, Figure S4A). To overexpress X26nt, BGCs were transfected with X26nt OE lentivirus and control lentivirus (control). Then, transfected BGCs were subcutaneously injected into the mice. Twenty-four days after injection, we harvested the subcutaneous tumors and found that the diameter, weight, and volume of the X26nt OE group were distinctly larger than those of the control group (Figure 7C, Figure S4B). In addition, X26nt overexpressing in BGCs promoted the proliferation of themselves compared with the control in vitro (Figure S4C,D).

Furthermore, we observed that knockdown X26nt increased VE-cadherin, which was distributed at the tumor edge, while overexpressing X26nt decreased VE-cadherin (Figure 7D,E). Finally, we found that suppression of X26nt significantly inhibited tubular formation, while the overexpression of X26nt induced tubular formation compared with the control group (Figure 7F). From these results, we concluded that GC-derived X26nt accelerates tumor growth and angiogenesis in vivo. Collectively, these results indicated that GC exosomal X26nt promotes HUVECs proliferation, migration, and tube formation via decreasing VE-cadherin, which facilitates angiogenesis (Figure 8).

4 | DISCUSSION

Emerging evidence indicated that exosomes were critically involved in GC progression including tumorigenesis, metastasis, angiogenesis, immune evasion, and drug resistance.³¹ In the current study, we first found that the X26nt of the shear product of XBP1u was highly expressed in GC serum exosomes. We further confirmed that X26nt derived from GC cell exosomes promoted the proliferation, migration, and tube formation of HUVECs. Exosomal X26nt can decrease VE-cadherin through binding to the 3'UTR of VE-cadherin mRNA, resulting in increasing vascular permeability. In vivo, we verified that X26nt accelerates the tumor growth and angiogenesis. Taken together, GC cell-derived exosomal X26nt facilitates the proliferation, migration, and tube formation of HUVECs and promotes tumor angiogenesis.

Hypoxia in the solid tumors induces splicing of XBP1u, then XBP1s translocates into the nucleus, binds to the specific sites in the promoters of target genes, and regulates tumor cells survival, immunoregulation, metastasis, and drug resistance.³² Our previous studies indicated that the XBP1s increased smooth muscle cell migration via PI3K/Akt activation and proliferation via downregulating calponin h1.³³ Although the current research focused on XBP1s, we found that X26nt was obviously upregulated in GC, suggesting that X26nt is possibly relevant in tumor growth and microenvironment formation. X26nt is likely to be degraded in normal tissue and low level of X26nt was found in normal serum in our study. So X26nt has been considered as an useless product of XBP1 splicing all along. For it is likely to be degraded in normal tissue and we also found low level of X26nt in normal serum. Our study may provide potential targets for GC therapy.

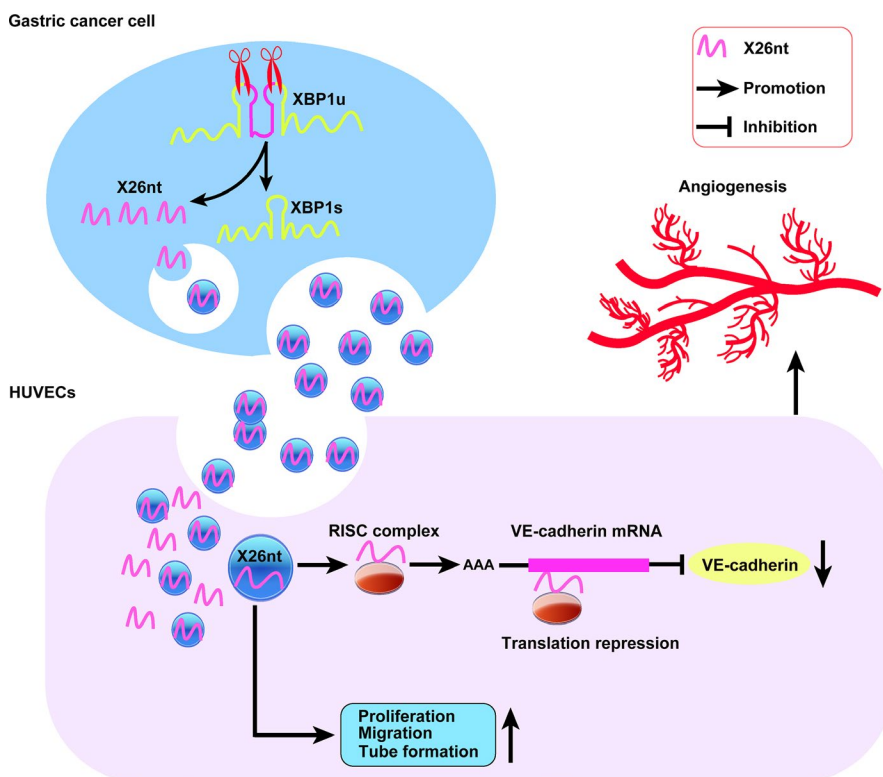


FIGURE 8 Schematic illustration of the mechanisms of gastric cancer (GC) cell exosomal X26nt-induced angiogenesis. Upon GC cell proliferation, the by-product X26nt, which is formed by XBP1u splicing, is secreted out through GC cell-derived exosomes. Exosomal X26nt binds to vascular endothelial cadherin (VE-cadherin) mRNA 3'UTR, which reduces the expression of VE-cadherin and promotes endothelial cell proliferation, migration, and tube formation, thereby promoting tumor angiogenesis

Exosomes are capable of mediating local and distant cell communication through transferring proteins, lipids, and nucleic acids during both physiological and pathological conditions.^{34,35} The ncRNAs in exosomes from GC cells were identified by deep sequencing. In recent years, the functions of exosomal ncRNAs on tumor angiogenesis have been gradually discovered. For example, miR-452 regulates cell proliferation, migration, and angiogenesis by suppressing vascular endothelial growth factor expression in early colorectal cancer progression.³⁶ In addition, secretory miRNAs are also involved in remodeling tumor microenvironment shaped and dominated by cancer cells.^{37,38} MiR-155 encapsulated by exosomes from GC can enhance the generation of new vessels for GC in vitro through inhibiting the expression of Forkhead box O3 protein.³⁹ The current study is the first, to our knowledge, to provide evidence for the effect of X26nt on angiogenesis in GC, suggesting X26nt, similar to microRNAs in length, as a crucial regulator of tumor angiogenesis. We found that GC cell-secreted exosomal X26nt increased the proliferation, migration, and tube formation of HUVECs. The ability of exosomes to package and transport ncRNAs is another basis for their participation in communication between cells.

Vascular endothelial-cadherin is an EC-specific adhesion molecule which has been reported to play a central regulatory role in the control of angiogenesis and endothelial barrier formation.¹² Growing evidence implicated that VE-cadherin participated in various aspects of vascular biology including EC migration,⁴⁰ survival,⁴¹ contact-induced growth inhibition,⁴² vascular integrity,⁴³⁻⁴⁵ and, most critically, ECs assembly into tubular structures.⁴⁶ In this study, we have demonstrated that GC cell-secreted exosomes are delivered to ECs and inhibit the expression of VE-cadherin, while removing X26nt from exosomes eliminates the exosome-induced decrease of VE-cadherin expression. As a result, we have found that GC cell-secreted exosomal X26nt increases the permeability. Our study also verified that X26nt could directly inhibit the expression of VE-cadherin of HUVECs by combining the 3'UTR of VE-cadherin mRNA, suggesting that GC cell-secreted exosomal X26nt increases the migration and tube formation of HUVECs and further promotes tumor angiogenesis by decreasing VE-cadherin. Consistently, previous study has shown that soluble E-cadherin-positive exosomes heterodimerize with VE-cadherin on ECs and promote angiogenesis in ovarian cancer.⁴⁷ Solid tumor vasculature is exceptionally variable in size and shape, and is not organized similarly to normal tissue due to the abnormal properties of tumor ECs.^{48,49} In tumor neovasculature, aberrant tumor vessels demonstrated that decreased levels of junctional VE-cadherin resulted in slack barrier connection and increased vascular permeability.^{50,51} Interestingly, in vivo study, VE-cadherin was found to be higher expressed inside of the tumor compared to that at the tumor edge in the X26nt OE group. Our study suggests that low expression of VE-cadherin facilitates ECs surrounding the tumor to migrate inside the tumor, form new blood vessels, and promote tumor growth. Further studies are needed to determine additional molecular mechanisms that might specifically facilitate X26nt-regulated angiogenesis in cancer.

In summary, we show that GC cell-secreted exosomal X26nt inhibits the expression of VE-cadherin in HUVECs and further promotes angiogenesis in vitro and in vivo, possibly a compensatory

mechanism to tumor angiogenesis. Our study also provides evidence that X26nt plays a key role in regulating angiogenesis in the tumor microenvironment. These results suggest novel mechanistic insights for understanding the role of X26nt in tumor angiogenesis.

ACKNOWLEDGMENTS

We thank our colleagues in the department of laboratory medicine for helpful discussions and valuable assistance. This study was supported in part by the National Natural Science Foundation of China (81802082 to JY, 81672363 to LS, and 81873863 to YZ), Shanghai "Rising Stars of Medical Talent" Youth Development Program-Clinical Laboratory Practitioners Program (2019016 to JY), Gao Yuan Development Program of Shanghai Municipal Education Commission; Key Specialty Development Program of Shanghai Municipal Health Commission.

DISCLOSURE

The authors have no conflict of interest.

ORCID

Lisong Shen  <https://orcid.org/0000-0002-6647-4749>

REFERENCES

1. Rawla P, Barsouk A. Epidemiology of gastric cancer: global trends, risk factors and prevention. *Prz Gastroenterol.* 2019;14:26-38.
2. Bray F, Ferlay J, Soerjomataram I, Siegel RL, Torre LA, Jemal A. Global cancer statistics 2018: GLOBOCAN estimates of incidence and mortality worldwide for 36 cancers in 185 countries. *CA Cancer J Clin.* 2018;68:394-424.
3. Song Z, Wu Y, Yang J, Yang D, Fang X. Progress in the treatment of advanced gastric cancer. *Tumour Biol.* 2017;39:1010428317714626.
4. de Mello RA, de Oliveira J, Antoniou G. Angiogenesis and apatinib: a new hope for patients with advanced gastric cancer? *Future oncology (London, England).* 2017;13:295-298.
5. Zhang W, Tan Y, Ma H. Combined aspirin and apatinib treatment suppresses gastric cancer cell proliferation. *Oncol Lett.* 2017;14:5409-5417.
6. Petrioli R, Francini E, Roviello F, et al. Sequential treatment with epirubicin, oxaliplatin and 5FU (EOF) followed by docetaxel, oxaliplatin and 5FU (DOF) in patients with advanced gastric or gastroesophageal cancer: a single-institution experience. *Cancer Chemother Pharmacol.* 2015;75:941-947.
7. Wagner AD, Unverzagt S, Grothe W, et al. Chemotherapy for advanced gastric cancer. *Cochrane Database Syst Rev.* 2010;Cd004064.
8. Chung HW, Lim JB. High-mobility group box-1 contributes tumor angiogenesis under interleukin-8 mediation during gastric cancer progression. *Cancer Sci.* 2017;108:1594-1601.
9. Kim J, Miranda AC, Popel AS, Green JJ. Gene delivery nanoparticles to modulate angiogenesis. *Adv Drug Deliv Rev.* 2017;119:20-43.
10. Tu T, Zhang C, Yan H, et al. CD146 acts as a novel receptor for netrin-1 in promoting angiogenesis and vascular development. *Cell Res.* 2015;25:275-287.
11. Bazzoni G, Dejana E. Endothelial cell-to-cell junctions: molecular organization and role in vascular homeostasis. *Physiol Rev.* 2004;84:869-901.
12. Warren NA, Voloudakis G, Yoon Y, Robakis NK, Georgakopoulos A. The product of the γ -secretase processing of ephrinB2 regulates VE-cadherin complexes and angiogenesis. *Cell Mol Life Sci.* 2018;75:2813-2826.
13. Ferrara N, Kerbel RS. Angiogenesis as a therapeutic target. *Nature.* 2005;438:967-974.

14. Spaan CN, Smit WL, van Lidth de Jeude JF, et al. Expression of UPR effector proteins ATF6 and XBP1 reduce colorectal cancer cell proliferation and stemness by activating PERK signaling. *Cell Death Dis.* 2019;10:490.
15. Kurywachak P, Kalluri R. An evolving function of DNA-containing exosomes in chemotherapy-induced immune response. *Cell Res.* 2017;27:722-723.
16. Chen Y, Xie Y, Xu L, et al. Protein content and functional characteristics of serum-purified exosomes from patients with colorectal cancer revealed by quantitative proteomics. *Int J Cancer.* 2017;140:900-913.
17. Hoshino A, Costa-Silva B, Shen TL, et al. Tumour exosome integrins determine organotropic metastasis. *Nature.* 2015;527:329-335.
18. Mathivanan S, Ji H, Simpson RJ. Exosomes: extracellular organelles important in intercellular communication. *J Proteomics.* 2010;73:1907-1920.
19. Hu Y, Rao SS, Wang ZX, et al. Exosomes from human umbilical cord blood accelerate cutaneous wound healing through miR-21-3p-mediated promotion of angiogenesis and fibroblast function. *Theranostics.* 2018;8:169-184.
20. Zhao W, Zheng XL, Zhao SP. Exosome and its roles in cardiovascular diseases. *Heart Fail Rev.* 2015;20:337-348.
21. Zhao N, Cao J, Xu L, et al. Pharmacological targeting of MYC-regulated IRE1/XBP1 pathway suppresses MYC-driven breast cancer. *J Clin Investig.* 2018;128:1283-1299.
22. Yang J, Xu J, Danniell M, et al. The interaction between XBP1 and eNOS contributes to endothelial cell migration. *Exp Cell Res.* 2018;363:262-270.
23. Zeng L, Xiao Q, Chen M, et al. Vascular endothelial cell growth-activated XBP1 splicing in endothelial cells is crucial for angiogenesis. *Circulation.* 2013;127:1712-1722.
24. Margariti A, Li H, Chen T, et al. XBP1 mRNA splicing triggers an autophagic response in endothelial cells through BECLIN-1 transcriptional activation. *J Biol Chem.* 2013;288:859-872.
25. Zeng L, Zampetaki A, Margariti A, et al. Sustained activation of XBP1 splicing leads to endothelial apoptosis and atherosclerosis development in response to disturbed flow. *Proc Natl Acad Sci USA.* 2009;106:8326-8331.
26. Leucci E, Patella F, Waage J, et al. microRNA-9 targets the long non-coding RNA MALAT1 for degradation in the nucleus. *Sci Rep.* 2013;3:2535.
27. Chen X, Li L, Liu F, Hoh J, Kapron CM. Cadmium induces glomerular endothelial cell-specific expression of complement factor H via the -1635 AP-1 binding site. *J Immunol.* 2019;202:1210-1218.
28. Hsu YL, Hung JY, Chang WA, et al. Hypoxic lung cancer-secreted exosomal miR-23a increased angiogenesis and vascular permeability by targeting prolyl hydroxylase and tight junction protein ZO-1. *Oncogene.* 2017;36:4929-4942.
29. Alam KJ, Mo JS, Han SH, et al. MicroRNA 375 regulates proliferation and migration of colon cancer cells by suppressing the CTGF-EGFR signaling pathway. *Int J Cancer.* 2017;141:1614-1629.
30. Xu B, Zhang Y, Du XF, et al. Neurons secrete miR-132-containing exosomes to regulate brain vascular integrity. *Cell Res.* 2017;27:882-897.
31. Fu M, Gu J, Jiang P, Qian H, Xu W, Zhang X. Exosomes in gastric cancer: roles, mechanisms, and applications. *Mol Cancer.* 2019;18:41.
32. Romero-Ramirez L, Cao H, Nelson D, et al. XBP1 is essential for survival under hypoxic conditions and is required for tumor growth. *Cancer Res.* 2004;64:5943-5947.
33. Zeng L, Li Y, Yang J, et al. XBP 1-deficiency abrogates neointimal lesion of injured vessels via cross talk with the PDGF signaling. *Arterioscler Thromb Vasc Biol.* 2015;35:2134-2144.
34. Zhang X, Shi H, Yuan X, Jiang P, Qian H, Xu W. Tumor-derived exosomes induce N2 polarization of neutrophils to promote gastric cancer cell migration. *Mol Cancer.* 2018;17:146.
35. Tkach M, Théry C. Communication by extracellular vesicles: where we are and where we need to go. *Cell.* 2016;164:1226-1232.
36. Mo JS, Park WC, Choi SC, Yun KJ, Chae SC. MicroRNA 452 regulates cell proliferation, cell migration, and angiogenesis in colorectal cancer by suppressing VEGFA expression. *Cancers.* 2019;11:1613.
37. Li L, Li C, Wang S, et al. Exosomes derived from hypoxic oral squamous cell carcinoma cells deliver miR-21 to normoxic cells to elicit a prometastatic phenotype. *Cancer Res.* 2016;76:1770-1780.
38. Ding G, Zhou L, Qian Y, et al. Pancreatic cancer-derived exosomes transfer miRNAs to dendritic cells and inhibit RFXAP expression via miR-212-3p. *Oncotarget.* 2015;6:29877-29888.
39. Zhou Z, Zhang H, Deng T, et al. Exosomes carrying microRNA-155 target forkhead box O3 of endothelial cells and promote angiogenesis in gastric cancer. *Mol Ther Oncolytics.* 2019;15:223-233.
40. Breviario F, Caveda L, Corada M, et al. Functional properties of human vascular endothelial cadherin (7B4/cadherin-5), an endothelium-specific cadherin. *Arterioscler Thromb Vasc Biol.* 1995;15:1229-1239.
41. Carmeliet P, Lampugnani MG, Moons L, et al. Targeted deficiency or cytosolic truncation of the VE-cadherin gene in mice impairs VEGF-mediated endothelial survival and angiogenesis. *Cell.* 1999;98:147-157.
42. Caveda L, Martin-Padura I, Navarro P, et al. Inhibition of cultured cell growth by vascular endothelial cadherin (cadherin-5/VE-cadherin). *J Clin Investig.* 1996;98:886-893.
43. Liao F, Li Y, O'Connor W, et al. Monoclonal antibody to vascular endothelial-cadherin is a potent inhibitor of angiogenesis, tumor growth, and metastasis. *Cancer Res.* 2000;60:6805-6810.
44. Corada M, Mariotti M, Thurston G, et al. Vascular endothelial-cadherin is an important determinant of microvascular integrity *in vivo*. *Proc Natl Acad Sci USA.* 1999;96:9815-9820.
45. Dejana E. Endothelial adherens junctions: implications in the control of vascular permeability and angiogenesis. *J Clin Investig.* 1997;100:S7-S10.
46. Bach TL, Barsigian C, Chalupowicz DG, et al. VE-Cadherin mediates endothelial cell capillary tube formation in fibrin and collagen gels. *Exp Cell Res.* 1998;238:324-334.
47. Tang MKS, Yue PYK, Ip PP, et al. Soluble E-cadherin promotes tumor angiogenesis and localizes to exosome surface. *Nat Commun.* 2018;9:2270.
48. Dudley AC. Tumor endothelial cells. *Cold Spring Harb Perspect Med.* 2012;2:a006536.
49. Baluk P, Hashizume H, McDonald DM. Cellular abnormalities of blood vessels as targets in cancer. *Curr Opin Genet Dev.* 2005;15:102-111.
50. Giannotta M, Trani M, Dejana E. VE-cadherin and endothelial adherens junctions: active guardians of vascular integrity. *Dev Cell.* 2013;26:441-454.
51. Mazzone M, Dettori D, de Oliveira RL, et al. Heterozygous deficiency of PHD2 restores tumor oxygenation and inhibits metastasis via endothelial normalization. *Cell.* 2009;136:839-851.

SUPPORTING INFORMATION

Additional supporting information may be found online in the Supporting Information section.

How to cite this article: Chen X, Zhang S, Du K, et al. Gastric cancer-secreted exosomal X26nt increases angiogenesis and vascular permeability by targeting VE-cadherin. *Cancer Sci.* 2021;112:1839-1852. <https://doi.org/10.1111/cas.14740>